# EFFICIENT HYBRID ACTUATION USING SOLID-STATE ACTUATORS

Final Report

Contract Number:     NAG-1-2190

Principal Investigators:

    Donald J. Leo
    Harley H. Cudney

    CIMSS / Mechanical Engineering Department
    Virginia Tech
    Blacksburg, VA 24061-0261
    (voice) 540.231.2917
    (fax) 540.231.2903
    donleo@vt.edu
    cudney@vt.edu

Subcontractor:

    Dynamic Structures and Materials, LLC
    Dr. Jeffrey Paine, Managing Partner
    309 Williams Square
    Franklin, TN 37064

Program Manager:

    Dr. Garnett Horner
    Structural Dynamics Branch
    Mail Stop 230
    4b West Taylor Street
    NASA Langley Research Center     Building 1293B, Room 104B
    Hampton, VA 23681

# Executive Summary

Piezohydraulic actuation is the use of fluid to rectify the motion of a piezoelectric actuator for the purpose of overcoming the small stroke limitations of the material. In this work we study a closed piezohydraulic circuit that utilizes active valves to rectify the motion of a hydraulic end affector. A linear, lumped parameter model of the system is developed and correlated with experiments. Results demonstrate that the model accurately predicts the filtering of the piezoelectric motion caused by hydraulic compliance. Accurate results are also obtained for predicting the unidirectional motion of the cylinder when the active valves are phased with respect to the piezoelectric actuator. A time delay associated with the mechanical response of the valves is incorporated into the model to reflect the finite time required to open or close the valves. This time delay is found to be the primary limiting factor in achieving higher speed and greater power from the piezohydraulic unit. Experiments on the piezohydraulic unit demonstrate that blocked forces on the order of 100 N and unloaded velocities of 180 $\mu$m/sec are achieved.

# Contents

# List of Figures

# 1 Introduction

Piezohydraulic actuation is the use of fluid in order to amplify or rectify the motion of a piezoelectric actuator. Piezoelectric devices are low displacement, high force actuators that often require motion amplification for use in applications which require strokes in the millimeter and centimeter range. The fundamental problem is the maximum strain of piezoelectric materials is on the order of 0.1%-0.4%, thus limiting the displacement of direct actuation devices. Typical free displacements of piezoceramic actuators operated in the $d_{33}$ mode is 10-100 $\mu$m.

The low stroke output of piezoelectric devices has motivated the development of novel actuator technologies that mechanically amplify the displacement at the expense of reduced force output. In a comprehensive overview of the technology to the mid-1990s, Near (1996) demonstrates that piezoelectric actuators are available in a wide range of force and stroke levels.

A concept that has recently gained attention is the use of frequency rectification to increase the stroke output of piezoelectric devices. Frequency rectification is the transformation of high-frequency, low-stroke motion to low-frequency, high-stroke motion. The concept of frequency rectification is not new. It is the operating principle of piezoelectric ultrasonic motors, electrohydraulic actuation systems, and, more generally, the fundamental concept behind AC-DC power conversion. Several patents exist utilizing the concept as the basis of inventions involving fluid-moving devices using piezoelectric materials. The recent interest in this concept for piezoelectric devices is derived from the realization that high-frequency

operation maximizes the power density and specific power of piezoelectric actuators. The challenge is to rectify the high-frequency, high power motion of the piezoelectric actuator to lower frequency without incurring significant losses in the overall system.

The concept of frequency-rectified, piezohydraulic actuation has been studied recently by several researchers. Probably the most significant demonstration of high-frequency operation is the work by Hagood, et al., on the development of micro-hydraulic transducers (Roberts et al., 2000; N.W. Hagood, *et al*, 2000). Macro-scale piezoelectric pumps have been developed by Mauck and Lynch utilizing a piezoelectric stack actuator and a valve-controlled hydraulic circuit (Mauck and Lynch, 1999, 2000).

Both micro-scale and macro-scale pumps require a hydraulic end affector to transform the fluid motion to mechanical work. In our paper, we consider the modelling and characterization of a complete piezohydraulic actuation system that consists of a piezoelectric actuator, a hydraulic transmission, and a hydraulic cylinder that transforms the hydraulic power to mechanical power. The goal of the paper is to develop a model which accurately predicts the mechanical response of our piezohydraulic actuation system under varying operating conditions.

# 2 System Overview

The piezohydraulic system developed for this contract is shown in Figure 1. It consists of a piezoelectric stack actuator (built by DSM) coupled to a hydraulic circuit. The motion of the fluid is controlled by the phasing of the stack motion with the opening and closing of a set of active valves. The active valves are electromagnetic, solenoid-type valves controlled using an external circuit. The output device for the piezohydraulic circuit is a 9.52 mm diameter hydraulic cylinder. An accumulator is required for filling and pressurizing the system. It is not required for operation.
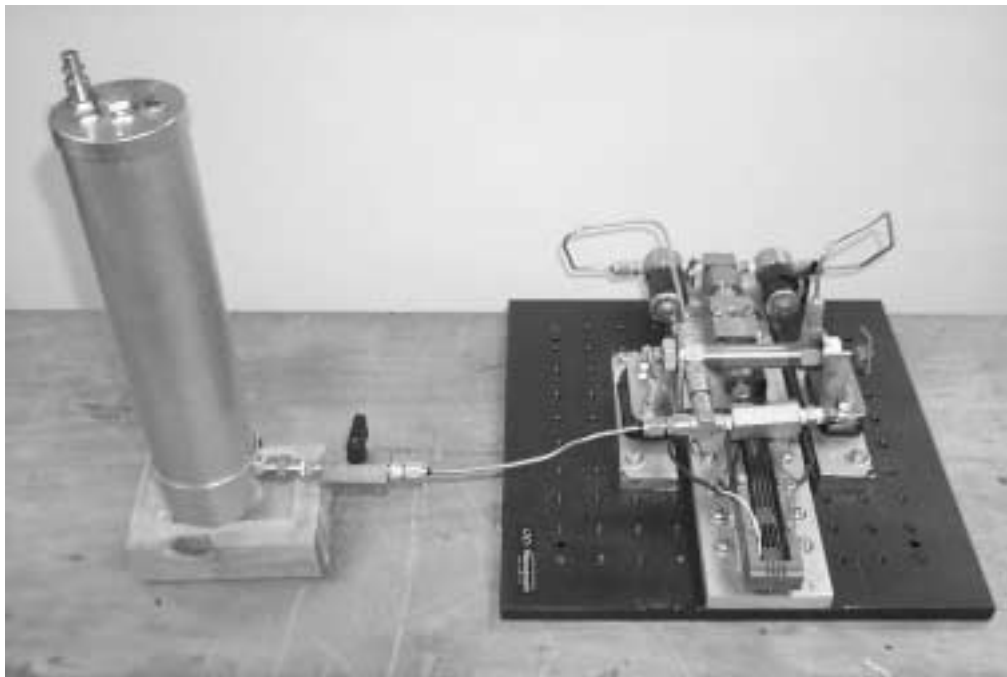


Figure 1: Piezohydraulic system

Control and power electronics for the piezohydraulic actuation system are separate. Small-signal control is provided by a digital signal processing (DSP) system (dSpace, Inc., Model Number 1102) with a graphical user interface. The DSP system is used to operate

the motion of the stack and the active valves. All user interfaces are coupled to Matlab©
for data processing and signal analysis.

The power electronics for the system are shown in Figure 2. Two generations of power
amplifiers were developed under this contract. The first generation is a three-channel am-
plifier with one channel (150 V, 1.5 A) and two lower-power channels. The three-channel
amplifier was designed for the purpose of controlling the stack and two active valves simulta-
neously. The second generation of the amplifier was a single channel (150 V, 1.5 A) amplifier
for controlling only the piezoelectric stack.



Figure 2: First (left) and second (right) generation power electronics.

The objective of this program was to develop energy efficient hybrid actuators consisting
of piezoelectric materials and hydraulic energy storage elements. The three primary areas
of development were

1. Concept development and benchtop verification

2. Piezohydraulic system modeling

3. Efficient power electronics design and fabrication

The results for each of these aspects of the contract are summarized below.

## Concept Development and Benchtop Verification

The piezohydraulic system shown in Figure 1 was designed, built, and tested during the period of performance for this contract. The system performance was measured to be 180 $\mu$m/sec velocity and a blocked force of 105 N. The primary limitations to achieving greater output power were determined to be the limited speed of response of the active valves and the compliance introduced by the mechanical structure of the actuator.

## Piezohydraulic system modeling

A lumped parameter model of the piezohydraulic system was developed and implemented in Matlab©. The model was correlated to experimental data and found to accurately predict the dynamic response of the hydraulic circuit and the unidirectional motion of the output cylinder.

## Efficient power electronics design and fabrication

The power electronics shown in Figure 2 were designed and built by Dynamic Structures and Materials, LLC, and tested by Virginia Tech. Both amplifiers were switching topologies designed to minimize the internal power dissipation.

## Recommendations for Future Work

Recommendations for future work include

- A more detailed design of the actuator and pumping chamber to minimize mechanical compliance. This will result in and increase in the output force.

- The design and fabrication of piezoelectric active valves to increase the operating speed of the system.

## Report Overview

The remainder of this report summarizes the modeling of the piezohydraulic actuation system and the tests for correlating the model with the experimental setup. The final section summarizes the performance of the benchtop system and discusses future improvements for obtaining increased power output.

# 3   Lumped Parameter Modeling of Piezohydraulic Systems

In a lumped parameter model, the fluid system is divided into lumped elements, with each element having mass and average parameters such as velocity and pressure. Then, the system equations are obtained by applying conservation of mass and Newton's Law to the element of fluid. This type of analysis is the approach taken by Doebelin (1972) and in similar derivations found in other texts, and it uses the fluid system elements of fluid resistance, capacitance (compliance) and inductance (inertance). The derivation of these elements from the governing equations of a fluid system is performed in Nasser Nasser (2000), and the various set of assumptions used to derive the lumped elements of fluid resistance, capacitance, and inertance are highlighted. Then these elements are used together to model one lump of fluid. As explained in detail in Nasser Nasser (2000), the model is expected to represent the dynamics of the fluid pipeline only when the density changes around an operating point are small. Furthermore, even though the system is essentially incompressible, the capacitive effect cannot be neglected as the operation or the excitation of the fluid is performed under high frequencies. Finally, the model is shown to accurately represent the dynamics of the piezohydraulic system developed.

The fluid elements of capacitance, resistance and inductance are obtained through the simplification of the governing equations of a fluid system and the comparison of the resulting equations with an analogous electrical system. In many cases electrical, mechanical and fluid systems can be described with equivalent differential equations and equivalent or analogous

Table 1: Force-Voltage Analogy.

| Mechanical | | Electrical | | Hydraulic | |
| --- | --- | --- | --- | --- | --- |
| $M$ | (mass) | $L$ | (inductance) | $I_f$ | (inductance) |
| $b$ | (damping) | $R$ | (resistance) | $R_f$ | (resistance) |
| $K$ | (stiffness) | $1/C$ | (1/capacitance) | $1/C_f$ | (1/compliance) |
| $x$ | (displacement) | $Q$ | (charge) | $\forall$ | (volume) |
| $\dot{x}$, | (velocity) | $i$ | (current) | $q$ | (flowrate) |
| $F$ | (force) | $\Delta V$ | (voltage) | $\Delta P$ | (pressure difference) |

variables. The result is that analogous systems have similar solutions and it is an additional tool that can be used to extend the solution of one particular system to all the analogous systems. This is done by using the same differential equations along with the corresponding analogous variables. However, there are two types of analogous systems. The force-current analogy "relates the analogous through- and across-variables of the electrical and mechanical systems", as described in Dorf and Bishop (1995). The second type of analogy is known as the force-voltage analogy, and it relates the velocity and current variables of a system.

Once the elements of fluid resistance, fluid inertance or inductance, and fluid compliance or capacitance are derived, then they are used to develop an equivalent electrical circuit to a lump of fluid. This equivalency is based on the force-voltage analysis, and the relationship between the analogous variables is shown in Table 1.

The analogous variables can then be used to construct equivalent differential equations among the analogous systems. Starting with the known components of the mechanical elements of damping, stiffness and inertia (mass), it is possible to obtain equivalent equations

in the electrical and fluid system with the use of the analogous variables. The result is shown in Table 2. Finally, the system analogy is used to obtain a mechanical system that is analogous to the electrical representation of a lump of fluid.

From the derivations performed in Nasser (2000), the fluid elements of capacitance, resistance, and inductance are defined and related to the mechanical variables in the following manner:

$$C_f = \frac{A\,l}{B} \sim \frac{1}{k} \quad , \quad \left[\frac{m^2\,m}{Pa} = \frac{m^5}{N}\right] \tag{1}$$

$$R_f = \frac{128\,\mu\,l}{\pi\,D^4}\left(1 + D\sum (l/d)_{eq}\right) \sim b \quad , \quad \left[\frac{N\,s}{m^2}\frac{m}{m^4} = \frac{Kg}{m^4\,s}\right] \tag{2}$$

$$I_f = \frac{\rho\,l}{A} \sim m \quad , \quad \left[\frac{\frac{Kg}{m^3}\,m}{m^2} = \frac{Kg}{m^4}\right] \tag{3}$$

These fluid elements are obtained through the use of the continuity equation, the energy equation and the equation for the conservation of momentum. By applying a certain set of assumptions for each case, each governing equation can be reduced to the form of the set of hydraulic equations shown in Table 2, where the constants are a function of pressure $(P)$, and either the flowrate $(q)$, its integral $(\int q\,dt)$, or its derivative $(dq/dt)$. These constants are then defined as either the fluid capacitance, fluid resistance or the fluid inductance. It is the fact that the capacitance, resistance and inertance are constant that makes a lumped parameter model linear. It approximates the behavior of the fluid around an operating point. Otherwise, the analysis of a fluid under general circumstances and not around a specific operating point would require a model incorporating a varying capacitance, resistance and/or inductance.

Using a local control volume, the general conservation of momentum equation is

Table 2: System Analogy

| System | Resistance/ Damping | Capacitance/ Stiffness | Inductance/ Mass |
|---|---|---|---|
| Mechanical | $F = C_b \dot{x}$ | $F = k\,x$ | $F = M \frac{d\vec{X}}{dt}$ |
| Electrical | $\Delta V = R\,i$ | $\Delta V = \frac{1}{C} \int i\, dt$ | $\Delta V = L \frac{di}{dt}$ |
| Hydraulic | $\Delta P = R_f\, q$ | $P = \frac{1}{C_f} \int q\, dt$ | $\Delta P = I_f \frac{dq}{dt}$ |

$$\sum \vec{F}_{cv} = \frac{\partial}{\partial t} \int_{cv} \vec{V} \rho \, d\forall + \int_{cs} \vec{V} \rho (\vec{V} \cdot \vec{n})\, dA \tag{4}$$

and by assuming that density and velocity are uniform within a lump, that changes in density with time are small around the operating point, and by assuming one dimensional flow, then the equation can be expressed as:

$$P_{n-1} - P_n = R_f\, q_n + \frac{\rho l}{A} \frac{dq_n}{dt} \tag{5}$$

where $n$ stands for the $n^{th}$ lump in a fluid pipeline. Using the definition of fluid inductance and dropping the subscripts for the $n^{th}$ lump, then the previous equation can be stated as:

$$\Delta P = R_f\, q + I_f \frac{dq}{dt} \tag{6}$$

Furthermore, by using the force-voltage analogy displayed in Table 1, the flowrate $q$ is equivalent to a current $i$, and the pressure difference $\Delta P$ is analogous to a voltage drop $\Delta V$. Then the previous equation becomes the total voltage drop across a resistor and an inductor in series (as shown in Figure 3a):
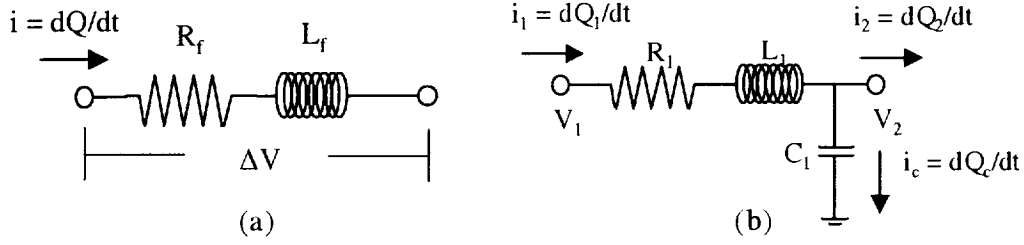
Figure 3: Model of a lump of fluid: (a) non-capacitive, and, (b) capacitive.

$$\Delta V = R_f\, i + I_f\, \frac{di}{dt} \tag{7}$$

This electrical circuit is valid for some fluid systems, where the storage due to compliance can be neglected. For example, this is the case when we consider the flow of fluid through a rigid pipe in a system where transients or minor changes from an average output does not matter. If we remember that the current is analogous to the flowrate, we see that the flowrate in, is equal to the flowrate out (which agrees with the simplified continuity equation when we assume negligible compliance).

In order to account for the compliance in a system, it is necessary to use a capacitor in the way it is shown in Figure 3b. This type of configuration has been used to model a lump of several fluid pipeline systems, such as water pipes, oil ducts, and arteries, among others. References include Streeter Streeter (1961) and Doebelin Doebelin (1972).

In Figure 3b, the current out, $i_2$, is not necessarily the same as the current in, $i_1$. It could be lower or even higher, depending on the charging or discharging of the capacitor. Thus, in the presence of compliance (modeled with a capacitor) there is some energy storage and/or release, and therefore the flowrates in and out of the lump are not equal. Nonetheless, it is important to realize that this model (Figure 3b) is different than the first one (Figure 3)

in one aspect. The first model is derived from the equation of conservation of momentum and satisfies the continuity equation. The second model results from the addition of the capacitive effect in order to simulate the compliance represented by the first term of the continuity equation. In addition, and as mentioned earlier, recall that the derivation of the fluid element of capacitance had a different set of assumptions than those used to obtain the fluid resistance and inductance (refer to Nasser (2000)). Thus, the result is a model that *approximates* the lump of fluid and the fluid dynamics in a pipeline.

Following the model of a lump of fluid (Figure 3b) then a hydraulic pipeline can be modeled as shown in Figure 4. The current source represents a flow source, and it is analogous to the case of an oscillating piston (which defines the flowrate through the pipeline).
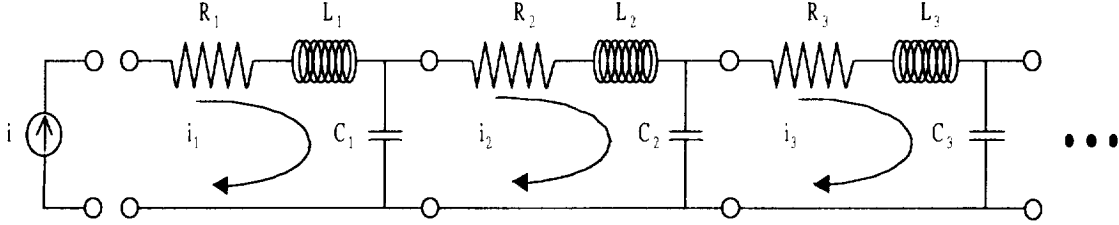


Figure 4: Analogous electrical model of a fluid pipeline.

The easiest way to analyze this circuit (for programming purposes) is to apply Kirchoff's voltage law (KVL). By applying KVL to each loop and expressing each voltage drop in terms of the charge, $Q$, then the following set of equations is obtained:

$$L_1\frac{d^2Q_1}{dt^2} + \frac{1}{C_1}(Q_1 - Q_2) + R_1\frac{dQ_1}{dt} = 0 \tag{8}$$

$$L_2\frac{d^2Q_2}{dt^2} + \frac{1}{C_2}(Q_2 - Q_3) + \frac{1}{C_1}(Q_2 - Q_1) + R_2\frac{dQ_2}{dt} = 0 \tag{9}$$

$$L_3 \frac{d^2 Q_3}{dt^2} + \frac{1}{C_3}(Q_3 - Q_4) + \frac{1}{C_2}(Q_3 - Q_2) + R_3 \frac{dQ_3}{dt} = 0 \tag{10}$$

Note that the current source, which represents the flow source, appears in the equation as the term $dQ_1/dt$. By using the force-voltage analogy shown in Table 1 it is possible to write an equivalent set of mechanical equations in terms of the elements of mass, spring and damping:

$$m_1 \ddot{x}_1 + k_1 (x_1 - x_2) + b_1 \dot{x}_1 = 0 \tag{11}$$

$$m_2 \ddot{x}_2 + k_2 (x_2 - x_3) + k_1 (x_2 - x_1) + b_2 \dot{x}_2 = 0 \tag{12}$$

$$m_3 \ddot{x}_3 + k_3 (x_3 - x_4) + k_2 (x_3 - x_2) + b_3 \dot{x}_3 = 0 \tag{13}$$

Then, by inspection of these equations, it is possible to construct a mechanical system that is analogous system to the electrical circuit model shown in Figure 4. The analogous mechanical system is shown in Figure 5.

Note that the input to the system, which represents the flow source, is $\dot{x}_1$, the velocity of the first lump (from the mechanical system standpoint). Recall that from the force-voltage analogy, a given flowrate is analogous to a given velocity in a mechanical system. Nonetheless, once the mechanical system is defined, then the input to the system may also be expressed in terms of a displacement, such as $x_1$, instead of the velocity, $\dot{x}_1$. Also note that if further lumps are to be added, then the next mass would be coupled to the stiffness $k_3$. Otherwise, the spring corresponding to the last lump (in this case the $3^{rd}$ lump) would be also coupled to ground. Thus Figure 5 represents a mechanical lumped parameter model of a fluid pipeline, with the elements of stiffness, damping and mass related to the electrical analogies of capacitance, resistance and inductance, respectively. Therefore, from equations (1), (2)

and (3), and from the force-voltage analogy shown in Table 1, the analogous stiffness, damping and mass for each lump of fluid is defined as:

$$k = A^2 \frac{1}{C_f} = \frac{A\,B}{l} \qquad , \qquad \left[\frac{N}{m}\right] \tag{14}$$

$$b = A^2\,R_f = 8\,\pi\,\mu\,\left(l + D\sum\left(l/d\right)_{eq}\right) \qquad , \qquad \left[\frac{Kg}{s}\right] \tag{15}$$

$$m = A^2\,I_f = \rho\,A\,l \qquad , \qquad [Kg] \tag{16}$$

Note that for equations (2) and (15) an area of $A = \frac{\pi}{4}\,D^2$ has been assumed.

In summary, the definitions stated in the set of equations (14), (15) and (16), along with the set of differential equations (11), (12) and (13), that describe the mechanical system shown in Figure 5, represent a three-lump model of the fluid system shown in Figure 6.

## Piezoelectric Actuator Model

For this work we will assume that the piezoelectric actuator is linear, that the electric field is applied only along one axis, and that the elongation of the stack is occuring in the same direction as the applied electric field. Under these assumptions, the electromechanical
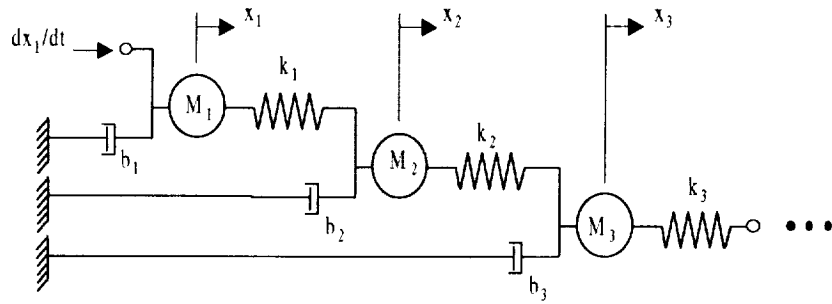


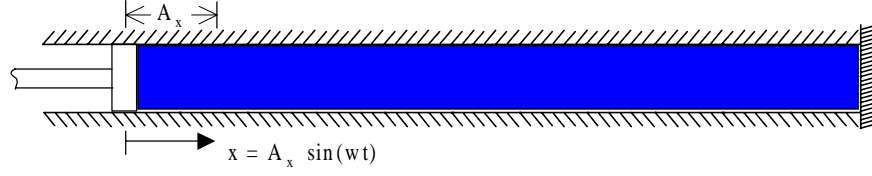Figure 5: Analogous mechanical model of a fluid pipeline.

Figure 6: Fluid-mechanical oscillating system.

relationships for the actuator can be written

$$Q_{pzt} = C_{pzt} V_{pzt} - x_o F_{pzt} \tag{17}$$

$$x_{pzt} = x_o V_{pzt} - \frac{1}{k_a} F_{pzt} \tag{18}$$

Under free operation, or no load, the stack does not exert any force and equation (18) reduces to $x_{pzt} = x_o V_{pzt}$. Thus, $x_{pzt}$ becomes the free displacement of the stack, it varies linearly with voltage, and it will be denoted as $x_{free}$. In the same manner, if the stack operates under a very large load, its output displacement $x_{pzt}$ is zero and equation (18) reduces to $F_{pzt} = k_a x_o V_{pzt}$. This is the blocked force of the PZT stack and it will be denoted as $F_{blkd}$. Furthermore, for the operation of the stack under the maximum voltage allowed, $V_{max}$, equation (18) can be rearranged in the form:

$$F_{pzt} = -k_a x_{pzt} + k_a x_o V_{max} \tag{19}$$

while the free displacement and the blocked force are expressed as:

$$x_{free} = x_o V_{pzt} \tag{20}$$

$$F_{blkd} = k_a x_o V_{pzt} \tag{21}$$

The rearranged constitutive equation (19) relates the force exerted by the piezo stack and its displacement to the voltage applied on it. Then equation (17) relates these parameters to the resulting charge. In fact, these equations represent a voltage controlled stack, meaning that it is controlled with a voltage input. It is the most general form of these expressions. Nonetheless, for a current controlled or a charge controlled system it is necessary to express equation (19) in terms of the charge across the piezo stack, $Q_{pzt}$. In order to do so, it is useful to solve equation (17) for the voltage across the piezoelectric stack:

$$V_{pzt} = \frac{Q_{pzt} - x_o F_{pzt}}{C_{pzt}} \tag{22}$$

Then by the substituting this expression into equation (19):

$$\begin{aligned} F_{pzt} &= k_a x_o \left( \frac{Q_{pzt}}{C_{pzt}} + \frac{x_o F_{pzt}}{C_{pzt}} \right) - k_a x_{pzt} \\ &= \frac{k_a x_o}{C_{pzt}} Q_{pzt} + \frac{k_a x_o^2}{C_{pzt}} F_{pzt} - k_a x_{pzt} \end{aligned} \tag{23}$$

and further manipulation yields to:

$$\begin{aligned} \left( 1 - \frac{k_a x_o^2}{C_{pzt}} \right) F_{pzt} &= \frac{k_a x_o}{C_{pzt}} Q_{pzt} - k_a x_{pzt} \\ F_{pzt} &= \left( \frac{\frac{k_a x_o}{C_{pzt}}}{\frac{C_{pzt} - k_a x_o^2}{C_{pzt}}} \right) Q_{pzt} - \left( \frac{k_a}{\frac{C_{pzt} - k_a x_o^2}{C_{pzt}}} \right) x_{pzt} \\ F_{pzt} &= \left( \frac{k_a x_o}{C_{pzt} - k_a x_o^2} \right) Q_{pzt} - \left( \frac{k_a C_{pzt}}{C_{pzt} - k_a x_o^2} \right) x_{pzt} \end{aligned} \tag{24}$$

where the term $C_{pzt} - k_a x_o^2$ is also known as the blocked capacitance of the piezoelectric stack, or $C_{blkd}$. Also, further substitution of the coefficients $F_1$ and $F_2$ for the coefficients of the previous equation, will reduce the expression to:

$$F_{pzt} = F_1 \, Q_{pzt} - F_2 \, x_{pzt} \tag{25}$$

where

$$F_1 = \frac{k_a \, x_o}{C_{pzt} - k_a \, x_o^2} \quad , \quad \left[\frac{N}{C}\right] \tag{26}$$

$$F_2 = \frac{k_a \, C_{pzt}}{C_{pzt} - k_a \, x_o^2} \quad , \quad \left[\frac{N}{m}\right] \tag{27}$$

Thus, equations (25) and (22) represent the set of constitutive equations for a charge controlled piezoelectric stack. Expressing the set of constitutive equations in terms of the force and the input variable (as done in equations (17) and (18) ) then the charge controlled equations for a piezoelectric stack become:

$$V_{pzt} = \left(\frac{1}{C_{pzt}}\right) Q_{pzt} - \left(\frac{x_o}{C_{pzt}}\right) F_{pzt} \tag{28}$$

$$x_{pzt} = \left(\frac{x_o}{C_{pzt}}\right) Q_{pzt} - \left(\frac{C_{pzt} - k_a \, x_o^2}{k_a \, C_{pzt}}\right) F_{pzt} \tag{29}$$

# 4   Piezohydraulic System Modeling

The lumped parameter modeling technique developed in the previous section is used to model two operating conditions for the piezohydraulic actuation system. The first operating condition is called *one-sided operation*. In this operating condition one of the active valves is closed and the other is open, allowing fluid to flow in only one direction through the hydraulic circuit. Exciting the piezoelectric actuator with an oscillatory input in this configuration results in oscillatory output of the hydraulic cylinder. One-sided operation is used to verify the parameters of the piezohydraulic model. The second operating condition is called *two-stage operation*. Two-stage operation occurs when the opening and closing of the active valves are timed with respect to the piezoelectric motion to produce unidirectional motion in the hydraulic cylinder. The direction of the motion is determined by the phasing of the valves relative to the piezoelectric actuator motion. The numerical models for these two operating conditions will be described in the following sections.

The lumped parameter techniques described in the previous section are used to determine a mass-spring-damper model for each component of the piezohydraulic system. The individual components are the stack and pumping chamber, side A of the hydraulic circuit, side B of the hydraulic circuit, and the hydraulic end affector. Lumped parameter modeling of each component yields a second-order equation of motion, as listed below:

$$
\begin{aligned}
\text{Stack and Chamber} \quad & M_{sc}\ddot{x}_{sc} + B_{sc}\dot{x}_{sc} + K_{sc}x_{sc} = F_{pzt} \\[4pt]
\text{SideA} \quad & M_A\ddot{x}_A + B_A\dot{x}_A + K_A x_A = 0 \\[4pt]
\text{SideB} \quad & M_B\ddot{x}_B + B_B\dot{x}_B + K_B x_B = 0 \\[4pt]
\text{End Affector} \quad & M_{ef}\ddot{x}_{ef} = 0
\end{aligned}
\tag{30}
$$

This set of equations can be combined into one matrix expression

$$\hat{M}\ddot{\hat{x}} + \hat{B}\dot{\hat{x}} + \hat{K}\hat{x} = \hat{F}Q_{pzt} \tag{31}$$

where $\hat{x} = \begin{bmatrix} x_{sc}^T & x_A^T & x_B^T & x_{ef}^T \end{bmatrix}^T$. At this point in the analysis the equations are completely

uncoupled. The coupling between the different components is introduced through a trans-

formation into a reduced set of coordinates. Defining the coordinates $x$ as the coordinates

of the coupled system, we can write a transformation between the $x$ and $\hat{x}$ as

$$\hat{x} = Tx \tag{32}$$

where $T$ is the transformation matrix between the uncoupled coordinates and the coordinates

of the coupled system. As such, the order of $x$ will be less than the order of $\hat{x}$ and the

transformation will be a nonsquare matrix. The equations of motion for the coupled system

can be found by applying the coordinate transformation,

$$M\ddot{x} + B\dot{x} + Kx = FQ_{pzt} \tag{33}$$

where $M = T^T\hat{M}T$, $B = T^T\hat{B}T$, $K = T^T\hat{K}T$, and $F = T^T\hat{F}$. A complete derivation of this

procedure is included in Nasser Nasser (2000).

## Modeling of the One-Sided Operation

One-sided operation is defined as the case in which one valve is always open and the other

valve is always closed. In this mode of operation, the boundary condition is reflected in the

transformation matrix T and a set of second-order differential equations like those shown in

equation (33) are used to simulate the motion of the end affector to an input waveform. As

discussed in the previous section, the amplifier electronics for the piezohydraulic system are current controlled. For any input frequency, the current across the stack is a constant value for the first half of the period and zero for the second half of the period. Thus, the waveform for the charge is a triangular wave at the same frequency.

Simulations are performed by placing the second-order equations into first-order form

$$\dot{z} = \begin{bmatrix} 0 & I \\ -M^{-1}K & -M^{-1}B \end{bmatrix} z + \begin{bmatrix} 0 \\ M^{-1}F \end{bmatrix} Q_{pzt}$$

$$y = Cz + DQ_{pzt}$$

(34)

where $y$ is a set of outputs, $C$ is the output matrix, and $D$ is a direct transmission matrix between the input charge and the outputs.

## Modeling of the Two-Stage Operation

The two-stage cycle operation uses two different one sided models in order to simulate the operation of the piezohydraulic unit. Assuming that for the first stage valve B is open while valve A is closed, then the corresponding one sided model (*Model B*) is developed and excited. Afterwards, a second one sided model is developed for the second stage (*Model A*), where valve A is open and valve B is closed. Notice that the models used in each stage have the same structure but they differ from one other. Thus, the set of states in the vector $\underline{x}$ for the first stage model is different than those for the second stage model. The input charge signal (which is proportional to the displacement of the piezoelectric stack) is also considered in two stages, one for the forward or forward stroke, and the other for the backward stroke.

After two-stages, one cycle is completed. By this time, the piston of the output cylinder has moved an amount $\Delta x$, and therefore the volume of fluid contained in each side of the

cylinder changes in proportion to this amount. Thus, after one cycle, the geometry of the lumps of fluid contained within the cylinder is updated and then the elements of mass, stiffness and damping are calculated again. This updating could be done after every stage, but it was not implemented in order to avoid further complexity in the program. Thus, the time-variance of the fluid system is modeled with a time-invariant lumped model, where the coefficients of the matrix equations change after one full cycle. Furthermore, the analysis of the dynamics of the entire system at both extreme cases, when the piston is at one end of the cylinder and then at the other end, revealed no considerable change. The poles, which represent the roots of the characteristic equation or the eigenvalues of the $A$ matrix, are a good indication of the dynamics of the system. When analyzed for both of the cases mentioned previously, their change in magnitude was less than 1%. This indicates that even though the dynamics associated with the cylinder itself do change (due to the displacement of the piston), the overall effect on the entire system coupled together is small and can be neglected.

Finally, since each stage consists of two different models, and therefore a different set of states, then at the beginning of each simulation for each state, a zero initial condition is used. Therefore, the initial condition response has been neglected and thus only the forced response is taken into account. This approach does not affect the correct prediction of the two-stage operation with a double-ended cylinder. The experimental measurements showed that the linear displacement of the hydraulic cylinder does not vary with time nor does it depend on the starting position of the piston itself. This is not the case though, for single-ended cylinders, for which further analysis is performed in Nasser Nasser (2000).

# 5   Numerical Analysis and Experimental Correlation

Two sets of experiments were performed to correlate the simulations of the piezohydraulic system with experimental results. The model of one-sided operation was verified by exciting the stack with an oscillatory signal and measuring the displacement of the hydraulic cylinder. The measured displacement was compared to the displacement predicted by the numerical simulation. The second set of experiments consisted of a two-stage operation of the piezohydraulic system for the purpose of verifying the ability of the model to predict the unidirectional motion of the hydraulic cylinder. Again, the displacement of the cylinder was measured and compared to the displacement predicted by the numerical model.

## One-sided Operation

The model of one-sided operation was verified by exciting the piezoelectric stack with oscillating waveforms of varying frequency and comparing the predicted response of the cylinder with its measured response. Current limitations on the amplifier precluded excitations above 100 Hz, therefore the frequency range of the studies was 5-100 Hz.

Figure 7 is a comparison of the measured and simulated response for 10, 50, and 90 Hz. At low frequencies we see that the response is predominantly a triangular wave with some ripple due to noise and external disturbances. We also see that the model accurately predicts both the shape and the peak-to-peak amplitude of the cylinder motion. Increasing the frequency to 50 Hz produces a distorted triangular wave. The correlation between the experimental and simulated data is still good but the model is not as accurate at this frequency as it

is at 10 Hz. The distortion in the waveform is attributed to the filtering effect of the hydraulic circuit between the piezoelectric stack and the hydraulic cylinder. The hydraulic line between the stack and the cylinder forms a mechanical filter which attenuates higher frequency components of the input signal. This conclusion is supported by the results of oscillating the stack at 90 Hz. At 90 Hz the displacement of the cylinder is predominantly sinusoidal due to the filtering of the higher harmonics of the input signal by the hydraulic circuit. The model accurately predicts this transition as well as the peak-to-peak amplitude of the output. These results demonstrate that the lumped parameter model is able to accurately predict the steady-state motion of the piezohydraulic system. Differences between the simulated and measured response are attributed to small inaccuracies of the model parameters, leading to errors in predicting the frequency response of the hydraulic circuit. The current experimental setup does not allow a frequency sweep with a sinusoidal excitation, therefore it is not possible to measure the resonance frequency of the piezohydraulic system. Frequency responses obtained from the model indicate that the resonance occurs at 158 Hz and the bandwidth of the actuator is approximately 240 Hz.

## Two-Stage Operation

Two-stage operation was verified by operating the piezohydraulic system with the active valves phased relative to the excitation of the piezoceramic actuator. The displacement of the hydraulic cylinder with no load was measured and compared to the displacement predicted by the model. The same parameters that were used to model one-sided operation were used to model the unidirectional motion of the cylinder. Figure 8 is a plot of the displacement of
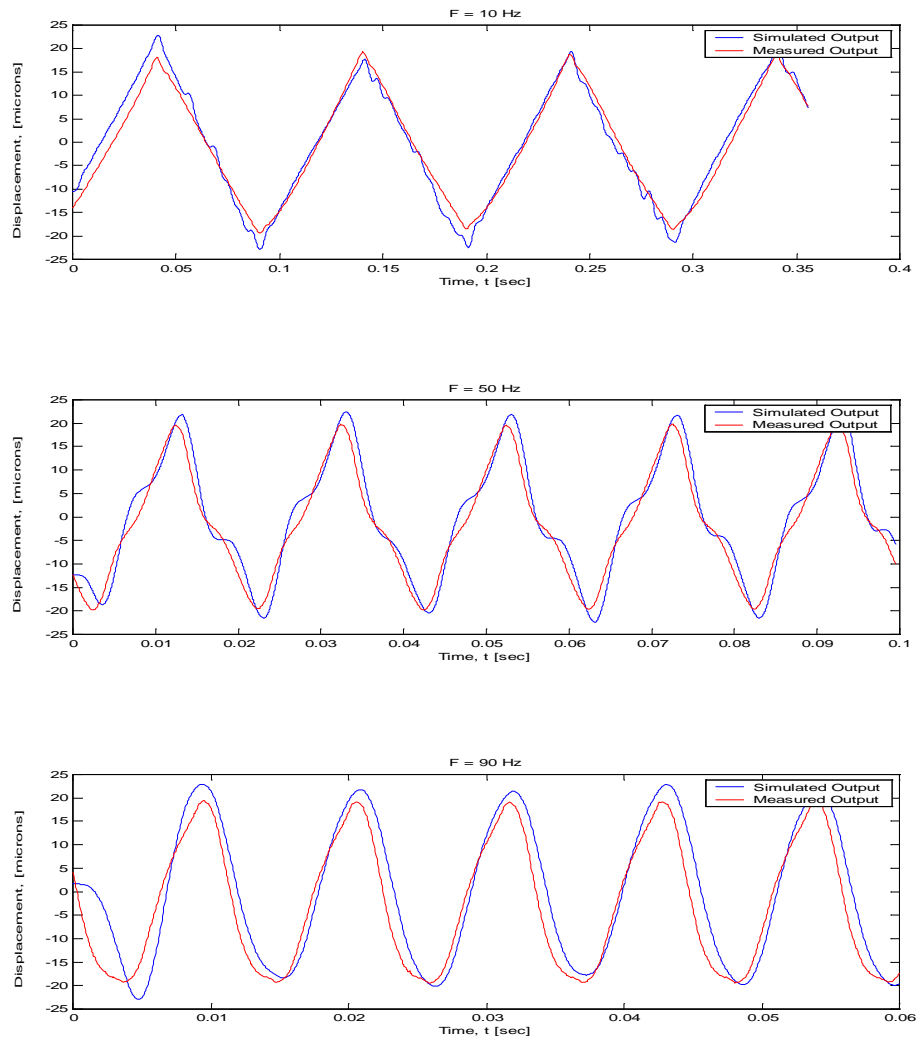
Figure 7: Measured and simulated time response comparison.

the hydraulic cylinder when operating the valves at 3 Hz. The key to achieving unidirectional

motion is the phasing of the valves relative to the motion of the piezoelectric stack. The valve

timing relative to the stack motion is shown in the diagram below the displacement plot.

When the stack is extending, valve A is opened to allow fluid to flow through one side of the

hydraulic circuit. The fluid flow moves the piston of the hydraulic cylinder and compresses

the fluid on the opposite side of the hydraulic circuit. Valve A is closed and valve B is opened

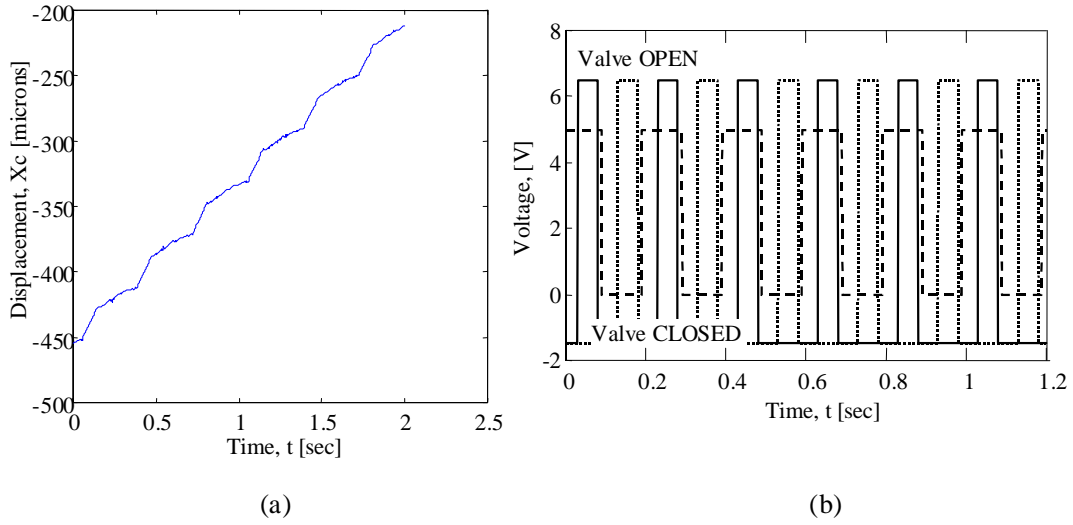(a)                                                              (b)

Figure 8: (a) Unidirectional cylinder motion at 3 Hz operation; (b) Timing diagram for the stack (dashed) and valves (solid/dotted).

while the stack is contracting. This allows fluid to flow from the B side of the circuit into the pumping chamber, resulting in motion of the hydraulic cylinder in the same direction as the first incremental displacement. Thus, each cycle of stack extension and contraction results in two incremental displacements of the hydraulic cylinder. Repeating this operation results in unidirectional motion of the hydraulic cylinder. Reversing the phasing of the valves changes the direction of the hydraulic cylinder.

The timing diagram in Figure 8 demonstrates an important aspect of the valve timing relative to the stack motion. Notice that there is a time in which both valves are closed during stack expansion or contraction. This aspect of the timing pattern serves two purposes. First, it allows pressure to build in the pumping chamber before fluid is allowed to flow in the hydraulic circuit. Secondly, it minimizes problems due to the finite transition time of the

active valves. Electrical and mechanical inertia in the active valves introduces a lag between the time at which the valve excitation is turned on (or off) and the opening (or closing) of the valve. Problems due to this time lag are evident in the cylinder motion when the frequency
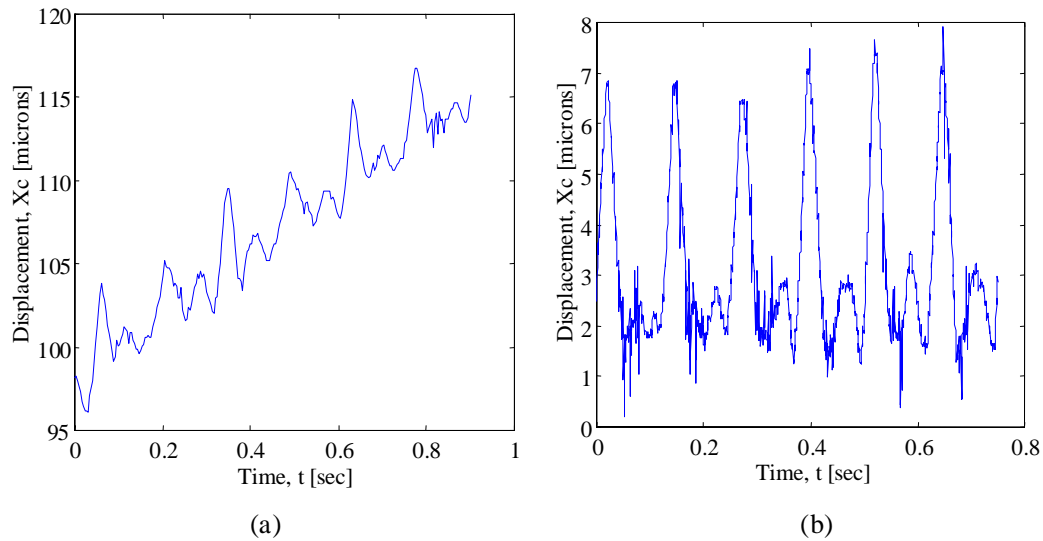


Figure 9: (a) Cylinder displacement for a pumping frequency of 7 Hz; (b) 8 Hz.

of the valve operation is increased. Figure 9a is a plot of the cylinder displacement for an operating frequency of 7 Hz. As with the 3 Hz operating frequency, extension of the stack causes forward motion of the hydraulic cylinder. Unlike the 3 Hz operating condition, though, the cylinder also exhibits a return, or 'springback', due to the fact that both valves are open simultaneously. This valve condition occurs because one valve is in the process of closing while the other valve is in the process of opening. Simultaneous opening of the valves opens the hydraulic circuit and the cylinder reverses its motion because the pressure begins to equalize throughout the system. This problem is more pronounced when operating the valves at a frequency of 8 Hz (see Figure 9b). At this operating condition, the forward

movement of the cylinder is almost completely canceled by the reverse motion caused by valve overlap.

The net result of valve overlap is a decrease in the operating speed of the hydraulic cylinder. Figure 10a is a plot of the measured speed of the hydraulic cylinder as a function of valve operating frequency. In the absence of valve overlap the speed would increase linearly with valve operating frequency. As Figure 10a demonstrates, the cylinder velocity does exhibit a linear increase from 1 Hz to 4 Hz. Above 4 Hz the cylinder speed begins to decrease due to overlap in the valves during two-stage operation. The maximum speed of 180 $\mu$m/sec is achieved at 6-7 Hz. A sharp decrease occurs at 8 Hz due to springback effect illustrated by Figure 9b.

The question remains as to whether the lumped parameter model can accurately predict the effects of valve overlap on the operating speed of the actuator. Here we introduce a model of valve overlap that effectively reduces the time that the stack is actuating the hydraulic cylinder. Valve overlap is modeled as a nulling of the charge input during the transition of the valve from open to closed configuration. Figure 10b is a plot of the predicted operating speed using the lumped parameter model that incorporates the effect of valve overlap. Comparing the result to Figure 10a demonstrates that the lumped parameter model with valve overlap accurately predicts the decrease in cylinder speed as a function of valve frequency. The curves are parameterized in terms of the transition time associated with the valve. A parametric study indicates that a transition time on the order of 60 milliseconds accurately predicts the decrease in operating speed for valve frequencies above 6 Hz. The model does not accurately model the sharp decrease that occurs when the valve frequency increases to 8 Hz. This

is due to the fact that the model of valve overlap does not include a model of the reverse

motion that occurs when both valves are open simultaneously. These results demonstrate
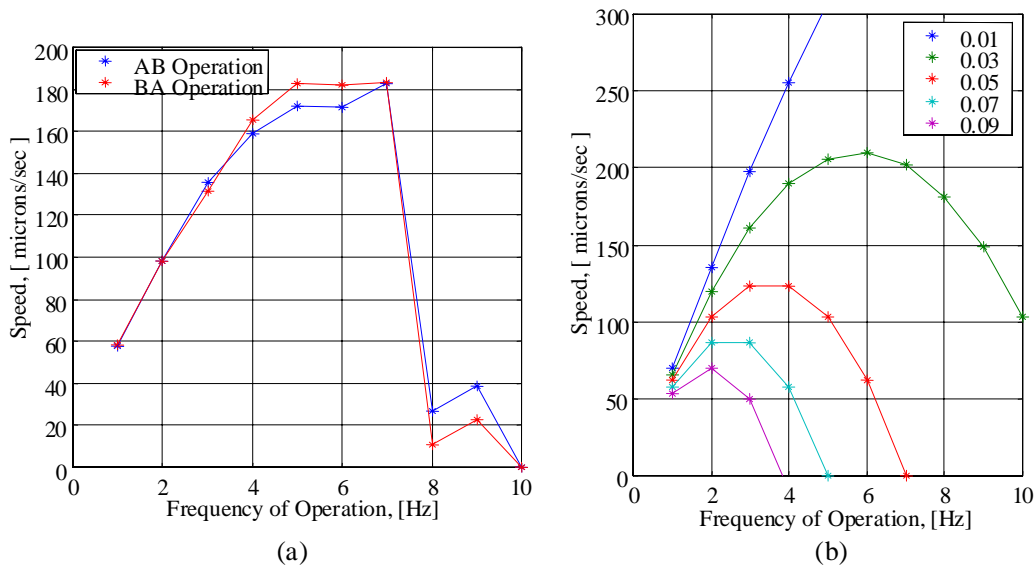


Figure 10: Cylinder velocity as a function of valve speed: (a) Measured; (b) Simulation.

that the lumped parameter model is able to accurately predict the unidirectional motion

of the hydraulic cylinder during two-stage operation. Experimental results demonstrate the

importance of valve overlap in reducing the output velocity of the hydraulic cylinder. The

lumped parameter model is also able to predict the reduction in speed, although the reverse

motion due to valve overlap is not modeled.

# 6   Final Results

The lumped parameter model of the piezohydraulic system is able to accurately predict the steady-state motion and unidirectional motion of the output cylinder. Modeling the hydraulic, mechanical, and electromechanical components separately and combining them via a coordinate reduction technique is an efficient means of developing the coupled equations of motion. The model is correlated to experimental results for oscillatory motion of the hydraulic cylinder with one valve closed and one valve open. These results demonstrate that the model accurately predicts the filtering effect of the hydraulic circuit on the output displacement of the hydraulic cylinder. The model is also verified using the piezohydraulic system for unidirectional actuation by phasing the active valves relative to the motion of the piezoelectric actuator. Accurate predictions of the maximum speed (180 $\mu$m/sec) and maximum operating frequency (7 Hz) are determined by incorporating a model of valve overlap into the coupled equations of motion. The transition time associated with the active valves was determined to be the limiting factor in achieving higher output velocities.

# 7   Acknowledgements

# References

Near, C. D., 1996, "Piezoelectric Actuator Technology," in *Proceedings of the Smart Structures and Materials Conference*, vol. 2717.

Roberts, D., Hagood, N., Carretero, J., Li, H., Mlcak, R., and Su, Y., 2000, "Piezoelectrically Driven Hydraulic Amplification Microvalve for High Pressure High Frequency Applications," in *Proceedings of the SPIE*, Paper Number 3985–59.

N.W. Hagood, *et al*, 2000, "Microhydraulic Transducer Technology for Actuation and Power Generation," in *Proceedings of the SPIE*, Paper Number 3985–81.

Mauck, L. and Lynch, C. S., 1999, "Piezoelectric Hydraulic Pump," in *Proceedings of the SPIE*, vol. 3668.

Mauck, L. and Lynch, C. S., 2000, "Piezoelectric Hydraulic Pump Development," in *Proceedings of the SPIE*, Paper Number 3985–85.

Doebelin, E., 1972, *System Dynamics Modeling and Response*, Bell & Howell Company, Columbus, Ohio.

Nasser, K. M., 2000, "Development and Analysis of the Lumped Parameter Model of a Piezohydraulic Actuator," Master's thesis, Virginia Polytechnic Institute and State University.

Dorf, R. and Bishop, R., 1995, *Modern Control Systems*, Seventh Edition, Addison-Wesley Publishing Company, Reading,Massachusetts.

Streeter, V., 1961, *Handbook of Fluid Dynamics*, First Edition, McGraw-Hill, New York.